A Conformational Switch in the Inhibitory γ-Subunit of PDE6 upon Enzyme Activation by Transducin†

Alexey E. Granovsky and Nikolai O. Artemyev*

Department of Physiology and Biophysics, University of Iowa College of Medicine, Iowa City, Iowa 52242

Received May 31, 2001; Revised Manuscript Received August 28, 2001

ABSTRACT: In response to light, a photoreceptor G protein, transducin, activates cGMP-phosphodiesterase (PDE6) by displacing the inhibitory γ-subunits (Pγ) from the enzyme's catalytic sites. Evidence suggests that the activation of PDE6 involves a conformational change of the key inhibitory C-terminal domain of Pγ. In this study, the C-terminal region of Pγ, Pγ-73−85, has been targeted for Ala-scanning mutagenesis to identify the point-to-point interactions between Pγ and the PDE6 catalytic subunits and to probe the nature of the conformational change. Pγ mutants were tested for their ability to inhibit PDE6 and a chimeric PDE5−conePDE6 enzyme containing the Pγ C-terminus-binding site of cone PDE. This analysis has revealed that in addition to previously characterized Ile^{86} and Ile^{87}, important inhibitory contact residues of Pγ include Asn^{74}, His^{75}, and Leu^{78}. The patterns of mutant PDE5−conePDE6 enzyme inhibition suggest the interaction between the PγAsn^{74}/His^{75} sequence and Met^{758} of the cone PDE6α′ catalytic subunit. This interaction, and the interaction between the PγIle^{86}/Ile^{87} and PDE6α′Phe^{777}/Phe^{781} residues, is most consistent with an α-helical structure of the Pγ C-terminus. The analysis of activation of PDE6 enzymes containing Pγ mutants with Ala-substituted transducin-contact residues demonstrated the critical role of PγLeu^{76}. Accordingly, we hypothesize that the initial step in PDE6 activation involves an interaction of transducin-α with PγLeu^{76}. This interaction introduces a bend into the α-helical structure of the Pγ C-terminus, allowing transducin-α to further twist the C-terminus thereby uncovering the catalytic pocket of PDE6.

In retinal rod and cone cells, visual heterotrimeric G proteins, transducins, couple photoexcitation of rhodopsin and cone opsins to marked activation of cGMP phosphodiesterases (PDE6 family) (*1*, *2*). In rod cells, the activity of the effector enzyme is inhibited in the dark as a result of the tight binding of two inhibitory γ-subunits (Pγ)[1] to the catalytic heterodimer, PDEα*β*. Cone holoPDE is comprised of a catalytic homodimer, $(PDE\alpha')_2$, and two cone Pγ subunits. Biochemical studies suggest that the inhibition of PDE6 involves a direct block of PDE catalytic site(s) by the C-terminal tail of Pγ (*3*, *4*). During the photoresponse, the activated GTP-bound transducin α-subunit (GtαGTP) interacts with and displaces the Pγ C-terminus from the active site(s). A recent crystallographic study revealed the structure of the C-terminal half of Pγ, Pγ-46−87, in a complex with Gtα (*5*). The structure provided the first molecular details about the mechanism of PDE activation by transducin. It shows that several C-terminal residues of Pγ interact with the switch II−α3-helix cleft of Gtα. It appears that Gtα induces a conformational change in Pγ allowing it to engage and occlude Pγ residues required for PDE inhibition. However, the nature of the conformational change in Pγ leading to PDE activation remains unclear since the conformation of Pγ in complex with the PDE6 catalytic subunits is unknown. Furthermore, although the inhibitory role of the Pγ C-terminus is well-established (*6*−*8*), the role of individual Pγ C-terminal residues has not been carefully examined.

An efficient expression system for the wild-type PDE6 has not yet been developed. PDE6 shares many common characteristics with cGMP-binding cGMP-specific PDE (PDE5) such as a common general domain organization, a high degree of homology of their catalytic domains, a strong substrate specificity for cGMP, and sensitivity to the same competitive inhibitors, zaprinast and dipyridamole (*9*). Furthermore, PDE5 can be readily expressed using the baculovirus/insect cell system. Therefore, our approach to studying the structure−function relationship of PDE6 has been to generate chimeras between PDE6 and PDE5 (*10*). A homodimeric catalytic cone PDE6α′ was selected as a PDE6 template for the construction of chimeric proteins to avoid complications arising from the heterodimeric nature of the rod enzyme. Recently, through Ala-scanning mutagenesis of a chimeric PDE5−PDE6α′ enzyme (Chi16) containing the Pγ-binding site (PDE6α′-737−784), we identified three Pγ contact residues on cone PDE6α′, Met^{758},

† This work was supported by National Institutes of Health Grants RO1 EY-10843 and EY-12682. NIH Grant DK-25295 supported the services provided by the Diabetes and Endocrinology Research Center of the University of Iowa. N.O.A. is an Established Investigator of the American Heart Association.

* To whom correspondence should be addressed. Telephone: (319) 335-7864. Fax: (319) 335-7330. E-mail: nikolai-artemyev@uiowa.edu.

[1] Abbreviations: PDE6α′ and PDE6α*β*, cone and rod cGMP phosphodiesterase catalytic subunits, respectively; Pγ, inhibitory γ-subunit of PDE6; tPDE6, PDE6 activated with limited trypsin digestion to remove Pγ subunits; PDE5, cGMP-binding, cGMP-specific PDE; ROS, rod outer segment(s); Gtα, rod G protein (transducin) α-subunit; R*, light-activated (bleached) rhodopsin; uROS, urea-stripped ROS membranes; GTPγS, guanosine 5′-*O*-(3-thiotriphosphate).

10.1021/bi011127j CCC: $20.00
Published on Web 10/12/2001

Phe^{777}, and Phe^{781} (*11*, *12*). A model of the PDE6α′ catalytic domain shows that Met^{758} and Phe^{777}/Phe^{781} are localized at opposite sides of the catalytic pocket perimeter (*12*). Moreover, the inhibition of mutant PDE5−PDE6α′ enzymes by Pγ mutants, PγI86A and PγI87A, indicated that Ile^{86} and Ile^{87} of Pγ interact with Phe^{777} and Phe^{78l} of PDE6α′ (*12*). These findings suggest a general orientation, but not a PDE6α′-bound conformation of the Pγ C-terminus. In this study, we have extended the Ala-scanning mutagenesis of the Pγ C-terminus to residues Pγ-73−85 to identify the point-to-point contacts with PDE6α′. A panel of C-terminal Pγ mutants has been tested for the inhibition of PDE6 activity and for the activation by transducin, when reconstituted with PDE6. On the basis of this analysis, we propose a model for the PDE6-bound structure of the Pγ C-terminus and hypothesize about the conformational rearrangement upon its interaction with transducin.

EXPERIMENTAL PROCEDURES

Materials. cGMP, GTPγS, and T4 DNA ligase were obtained from Roche Molecular Biochemicals. [^{3}H]cGMP was a product of Amersham Pharmacia Biotech. All restriction enzymes were purchased from New England Biolabs. AmpliTaq DNA polymerase was a product of Perkin-Elmer. TPCK-treated trypsin was from Worthington. All other reagents were purchased from Sigma or Fisher.

Preparation of tPDEα′, tPDEαβ, GtαGTPγS, and uROS Membranes. Bovine rod outer segment (ROS) membranes were obtained according to the method of Papermaster and Dreyer (*13*). Urea-stripped ROS membranes were prepared as described previously (*14*). HoloPDE6αβ and holoPDE6α′ were purified from outer segments according to the established protocols (*15*, *16*). Trypsin-treated PDEs (tPDEαβ and tPDEα′) were prepared as described previously (*17*). Limited proteolysis of native PDE6 with trypsin removes Pγ and activates the enzyme (*17*). GtαGTPγS was extracted from ROS membranes using GTPγS and purified as described previously (*18*). Purified proteins were stored in 40% glycerol at −20 °C.

Expression and Purification of Chi16 and Chi16 Mutants. Recombinant His$_6$-tagged Chi16 and its mutants (M758A, F777A, and F781A) were expressed in Sf9 cells and partially purified using affinity chromatography on a His-Bind resin (Novagen) as described previously (*12*). Purified proteins were dialyzed against 40% glycerol and stored at −20 °C.

Cloning and Preparation of Pγ Mutants. Pγ mutants were generated using the pET11a-Pγ expression vector (*8*, *19*). Construction of Pγ mutants (PγG85A, PγI86A, and PγI87A) was described previously (*8*, *12*). Pγ residues at positions 73−81, 83, and 84 were substituted with alanine using PCR-directed mutagenesis. A forward PCR primer contained an *Nde*I site. Reverse PCR primers contained a mutated codon and a *Sac*I site for substitutions of residues 73−76 or a *Bam*HI site for all other substitutions. PCR products were digested with a *Nde*I−*Bam*HI or *Nde*I−*Sac*I fragment and subcloned into the pET11a-Pγ vector cut with the corresponding enzymes. Sequences of all mutants were verified by automated DNA sequencing at the University of Iowa DNA Core Facility. Pγ and its mutants were expressed in *Escherichia coli* and purified on a SP-Sepharose fast flow column and on a C-4 HPLC column (Microsorb-MW, Rainin) as described previously (*19*). Purified proteins were lyophilized, dissolved in 20 mM HEPES buffer (pH 7.5), and stored at −80 °C until they were used.

PDE Activity Assay. PDE activity was measured using [^{3}H]-cGMP as described previously (*20*, *21*). Less than 15% of the cGMP was hydrolyzed during these reactions. The K_i values for inhibition of PDE activity by Pγ or mutants were measured using 1 pM tPDEαβ or tPDEα′, or 50−100 pM recombinant PDEs (Chi16 and mutants), in the presence of 4 or 0.5 μM cGMP, respectively (i.e., <35% of the K_m value for the respective PDEs) (*9*, *11*). In PDE activation experiments, 50 pM tPDEαβ was reconstituted with Pγ or its mutants to achieve a 95% inhibition of cGMP hydrolytic activity. The reconstituted enzyme was mixed with different amounts of GtαGTPγS (0.05−5 μM) in the presence of uROS membranes (1 μM rhodopsin). Reactions were initiated with the addition of 120 μM [^{3}H]cGMP.

Other Methods. Protein concentrations were determined by the Bradford method (*22*) using IgG as a standard, or by using calculated extinction coefficients at 280 nm. Concentrations of Chi16 and mutatnts were calculated on the basis of the fraction of PDE protein in preparations, and the molecular mass of 186 kDa for the PDE5 catalytic dimer. The fractional concentrations of PDE were determined from analysis of the Coomassie Blue-stained SDS gels using a HP ScanJet II CX/T scanner and Scion Image Beta 4.02 software. A typical fraction of Chi16 and its mutants in partially purified preparations was 10−15%. SDS−PAGE was performed by the Laemmli method (*23*) in 10−14% acrylamide gels. For Western immunoblotting, proteins were transferred to nitrocellulose (0.1 μm, Schleicher & Schuell) and analyzed using rabbit His probe (H-15) or sheep anti-PDE6α′ antibodies (*10*, *24*). The antibody−antigen complexes were detected using anti-rabbit or anti-goat/sheep IgG conjugated to horseradish peroxidase and ECL reagent (Pharmacia Biotech). The K_i values in Figures 1 and 2 and Table 1 were calculated by fitting the data to eq 1

$$Y = \frac{I_{max}}{1 + 10^{X - \log K_i}} \quad (1)$$

where I_{max} is the maximal inhibition and X is the total concentration of Pγ or Pγ mutants. Concentrations of PDE6 and recombinant chimeric PDEs used in inhibition experiments were 15−200-fold lower than the observed K_i values. Therefore, the maximal corrections of the K_i values using free Pγ concentrations could not exceed 5%. The K_a values in Figure 3 were calculated by fitting the data to eq 2

$$Y = \frac{A_{max}}{1 + 10^{\log K_a - X}} \quad (2)$$

where A_{max} is the maximal increase in PDE activity and X is the concentration of GtαGTPγS. Fitting the experimental data to equations was performed with nonlinear least-squares criteria using GraphPad Prizm Software. The K_i and K_a values are expressed as means ± standard error for three independent measurements.

RESULTS AND DISCUSSION

Analysis of PDE Inhibition by C-Terminal Mutants of Pγ. Approximately 11−17 C-terminal residues of Pγ are essential

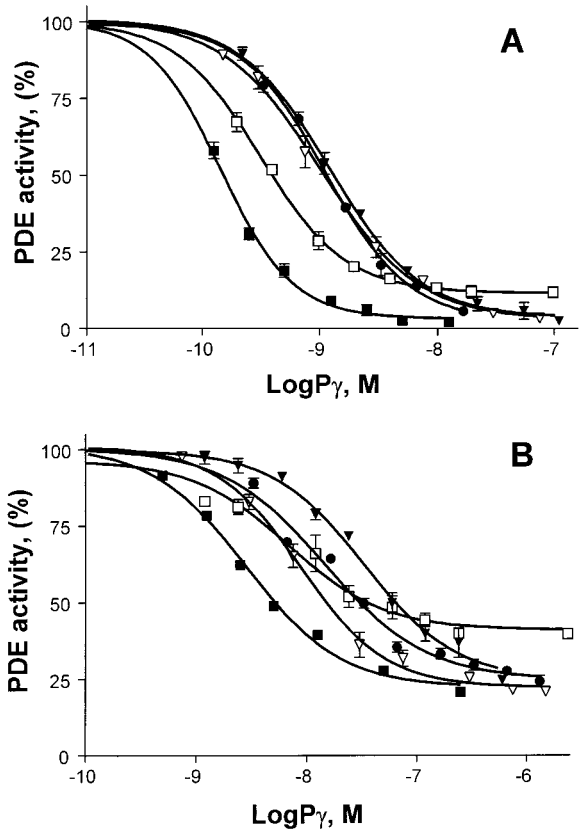

FIGURE 1: Effects of Pγ and Pγ mutants on the catalytic activity of tPDE6α' and Chi16. (A) Inhibition of tPDE6α' by Pγ (■), PγN74A (□), PγH75A (▼), PγL78A (▽), and PγG85A (●). The activity of tPDEα' (1 pM) was determined upon addition of increasing concentrations of Pγ or mutants using 4 μM cGMP. The K_i values (nanomolar) calculated from the inhibition curves were 0.14 ± 0.02 (■), 0.31 ± 0.05 (□), 1.2 ± 0.1 (▼), 1.0 ± 0.2 (▽), and 1.3 ± 0.3 (●). (B) Inhibition of Chi16 activity by Pγ (■), PγN74A (□), PγH75A (▼), PγL78A (▽), and PγG85A (●). The activity of Chi16 (50 pM) was determined upon addition of increasing concentrations of Pγ or mutants using 0.5 μM cGMP. The K_i values (nanomolar) calculated from the inhibition curves were 2.9 ± 0.2 (■), 4.9 ± 0.6 (□), 33 ± 6 (▼), 9.6 ± 0.9 (▽), and 14 ± 2 (●).

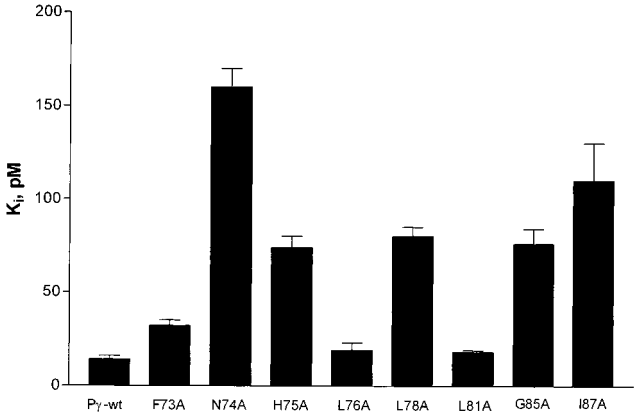

FIGURE 2: Inhibition of tPDE6$\alpha\beta$ by C-terminal mutants of Pγ. PDE activity was measured using [^{3}H]cGMP (*19*). The K_i values for inhibition of tPDE6$\alpha\beta$ activity (1 pM) by Pγ and Pγ mutants were determined in the presence of 4 μM cGMP. The results are presented as means ± the standard error for three independent measurements.

for the inhibition of PDE6 activity, as demonstrated by a progressive loss of inhibitory function in the C-terminally truncated Pγ mutants (*8*). Earlier, our analysis of the inhibition of mutant PDE5−PDE6α' enzymes by the Pγ mutants, PγI86A and PγI87A, has indicated that the PγIle^{86}/Ile^{87} sequence interacts with the PDE6α'Phe^{777}/Phe^{781} sequence (*12*). To further elucidate the point-to-point contacts between PDEα' and Pγ, Pγ residues within the Pγ-73−85 fragment, except Ala^{82}, have been targeted for Ala-scanning mutagenesis. The PγG85A mutant was included to assess the potential role of a conformational freedom that Gly^{85} may provide to the C-terminal PγIle^{86}/Ile^{87} sequence.

The Ala-substituted mutants of Pγ were examined for their ability to inhibit cGMP hydrolytic activities of cone PDE6α' and a chimeric PDE5−PDE6α' enzyme, Chi16 (*11*). Chi16 contains the Pγ C-terminus binding site, PDE6α'-737−784. Cone PDE6 devoid of the Pγ subunits (tPDE6α') was prepared using limited tryptic digestion of cone holoPDE6. This allows us to test the effects of Pγ mutants on PDE6α' activity. Substitutions of residues Phe^{73}, Leu^{76}, His^{79}, Leu^{81}, Gln^{83}, and Tyr^{84} did not significantly alter the Pγ inhibitory characteristics of tPDE6α' (Table 1). Modest increases in the K_i values were observed for E77A and E80A. The inhibitory defect of the N74A mutant is revealed in the

Table 1: Inhibition of tPDE6α', Chi16, and Its Mutants by Pγ C-Terminal Mutants[a]

	tPDE6α'	Chi16	F777A	F781A	M758A
Pγ	0.14 ± 0.02 (100)	2.9 ± 0.2 (85)	19 ± 2 (45)[b]	31 ± 5 (65)[b]	97 ± 10 (75)[b]
PγF73A	0.21 ± 0.02 (100)	2.3 ± 0.5 (85)			
PγN74A	0.31 ± 0.05 (90)	4.9 ± 0.6 (60)	<20%	43 ± 3 (35)	82 ± 9 (45)
PγH75A	1.2 ± 0.1 (100)	33 ± 6 (75)	98 ± 7 (40)	114 ± 16 (55)	103 ± 9 (65)
PγL76A	0.18 ± 0.02 (100)	2.2 ± 0.2 (85)			
PγE77A	0.46 ± 0.08 (100)	4.9 ± 0.5 (90)			
PγL78A	1.0 ± 0.2 (100)	9.6 ± 0.9 (80)	37 ± 5 (45)	30 ± 4 (60)	120 ± 15 (75)
PγH79A	0.28 ± 0.05 (100)	12 ± 3 (90)			
PγE80A	0.37 ± 0.07 (100)	4.1 ± 0.2 (85)			
PγL81A	0.29 ± 0.03 (100)	8.2 ± 0.5 (85)			
PγQ83A	0.26 ± 0.3 (100)	5.4 ± 3 (80)			
PγY84A	0.33 ± 0.6 (100)	3.3 ± 1 (85)			
PγG85A	1.3 ± 0.3 (100)	14 ± 2 (80)	26 ± 6 (40)	39 ± 3 (55)	112 ± 16 (65)
PγI86A	0.75 ± 0.08 (95)[b]	13 ± 1 (65)[b]	96 ± 13 (45)[b]	49 ± 8 (40)[b]	<20%[b]
PγI87A	0.65 ± 0.04 (100)[b]	6.6 ± 1.0 (70)[b]	64 ± 8 (25)[b]	32 ± 2 (55)[b]	<20%[b]

[a] PDE activity was measured using [^{3}H]cGMP (*19*). The K_i values for inhibition of tPDE6α' (1 pM) or recombinant PDEs (50−100 pM) by Pγ and Pγ mutants were determined using 4 and 0.5 μM cGMP as a substrate, respectively. The maximal effects of PDE inhibition by Pγ mutants (in parentheses) were determined using 10 μM Pγ or mutant. The results are presented as means ± the standard error for three independent measurements. [b] The data are from ref *12*.

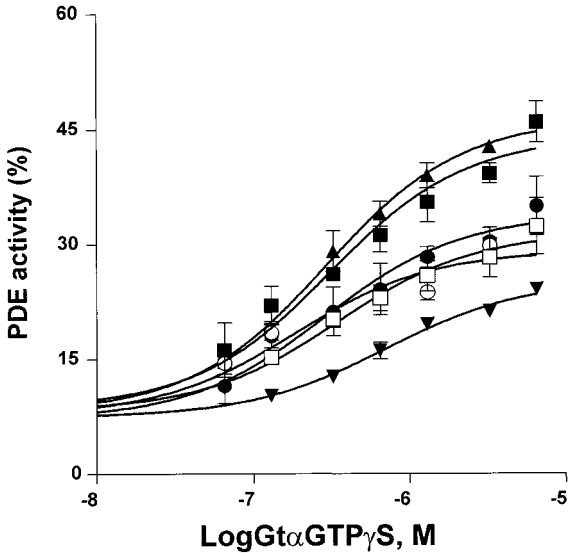

FIGURE 3: Activation of Pγ mutant-reconstituted tPDE6αβ by GtαGTPγS. tPDE6αβ (50 pM) was reconstituted with Pγ (■), PγF73A (□), PγL76A (▼), PγL78A (○), PγL81A (●), or PγI87A (▲) and mixed with uROS membranes (1 μM rhodopsin). The basal PDE activity of reconstituted enzymes was 5% of that for tPDE6αβ alone. GtαGTPγS (0.05−5 μM) was added to the mixtures, and reactions were initiated by addition of 120 μM cGMP. PDE activity is expressed as a percentage of tPDE6αβ activity [3200 mol of cGMP (mol of PDE)$^{-1}$ s^{-1}]. The calculated K_a values (nanomolar) and maximum effects (%) are as follows: 310 ± 44 and 44% (■), 347 ± 63 and 31% (□), 707 ± 126 and 25% (▼), 220 ± 45 and 29% (○), 290 ± 43 and 34% (●), and 295 ± 59 and 46% (▲), respectively.

incomplete inhibition of tPDE6α′ (~90%) and Chi16 (~60%) (Figure 1 and Table 1). Three Pγ mutations (H75A, L78A, and G85A) more significantly affected the ability of Pγ to inhibit tPDE6α′ and Chi16 as seen from the considerable increases in the K_i values (Figure 1). The H75A substitution caused a more than 10-fold increase in the K_i values for both tPDE6α′ (K_i = 1.2 nM) and Chi16 (K_i = 33 nM) (Table 1). The replacements of Leu[78] and Gly[85] increased the K_i values for PDE6α′ by ~10-fold and the K_i values for Chi16 by 3−4-fold (Figure 1 and Table 1). The Pγ mutants with substantially impaired inhibition of tPDE6α′ (N74A, H75A, L78A, and G85A) have been additionally examined for the inhibition of rod tPDE, tPDE6αβ (Figure 2). All these mutations led to a diminished capacity of Pγ to inhibit rod PDE. Interestingly, the N74A substitution resulted in a more profound deficiency of inhibition toward rod tPDE6αβ then for cone tPDE6α′ (Table 1 and Figure 2). Not only was the inhibition of tPDE6αpc by PγN74A incomplete, but the affinity was also reduced by more than 10-fold (Figure 2).

Mapping Point-to-Point Interactions between Pγ and PDE6α′. Impaired Pγ mutants (N74A, H75A, L78A, and G85A) have been further tested for their effects on the activity of Chi16 mutants. If a C-terminal residue of Pγ interacts with one of the three PDE6α′ residues (Met[758], Phe[777], or Phe[781]), the corresponding mutant of Chi16 is predicted to be inhibited comparably by Pγ and by the Pγ mutant. Other mutants of Chi16 would be less potently inhibited by the Pγ mutant than by the wild-type Pγ.

The patterns of inhibition of Chi16 mutants by the C-terminal mutants of Pγ are most consistent with Asn[74] and/or His[75] being the contact residues for Met[758] of PDE6α′. PγH75A inhibited Chi16M758A in a manner similar to that of wild-type Pγ, but had increased K_i values for inhibition of the F777A and F781A Chi16 mutants. Although partial inhibition complicates interpretation of the data for N74A, the mutant inhibited M758A with a K_i analogous to that of Pγ. The ability of PγN74A to inhibit F777A and F781A was impaired, indicative of a potential contact with Met[758]. Despite the defect caused by the L78A mutation for the inhibition of tPDE6α′, the effect was not as strong with Chi16 and its mutants. Perhaps Leu[78] interacts with a PDE6α′ residue, which is substituted by a nonconserved PDE5 residue in Chi16. The G85A mutation, while causing a significant impairment of the Pγ interaction with PDE6α′, also had a smaller effect on the inhibition of Chi16 and its mutants (Table 1). This suggests that the requirement for the flexibility of the Pγ C-terminal residues becomes greater when the binding of Pγ is tighter.

Activation of PDE6αβ Reconstituted with C-Terminal Pγ Mutants by Transducin. The crystal structure of the Pγ C-terminus bound to Gtα shows five transducin contact residues within the Pγ-73−87 region, Phe[73], Leu[76], Leu[78], Leu[81], and Ile[87] (*5*). To assess the role of the individual Pγ residues in PDE6 activation by transducin, we analyzed the ability of GtαGTPγS to stimulate rod tPDE6αβ reconstituted with Pγ mutants carrying Ala substitutions of the contact residues. Rod PDE6αβ rather then cone PDE6 was used in the activation experiments, because in contrast to the cone components, rod Gt and rod disk membranes were more readily available. Pγ mutants were added to 50 pM tPDE6αβ (100 pM PDE6 catalytic subunit) to produce a 95% inhibition of PDE activity. The K_i values for inhibition of tPDEαβ by the Pγ mutants utilized in the PDE activation assay are shown in Figure 2. tPDE6αβ reconstituted with wild-type Pγ served as a control. The Pγ mutant−tPDE6αβ complexes were mixed with uROS membranes containing 1 μM rhodopsin. The cGMP hydrolytic activity of reconstituted PDEs was measured upon addition of increasing concentrations of GtαGTPγS. The K_a values and maximal stimulated PDE activity levels were determined from the dose-dependent activation curves (Figure 3). The K_a value for the PDE complex containing wild-type Pγ was 310 nM, and the maximal stimulated PDE activity was 44% of the tPDE6αβ activity. Mutations of Phe[73], Leu[78], and Leu[81] impaired the ability of transducin to activate reconstituted enzymes, as evident from the reduced maximal levels of stimulated PDE activity (Figure 3). A particularly serious defect for tranducin activation was caused by the L76A mutation. The defect is apparent in both the increase in the K_a value and the reduction in the maximal level of stimulation (25% of tPDE6αβ activity). Unexpectedly, the activation of tPDE6αβ reconstituted with I87A was unaffected.

Activation of PDE6 by Transducin Requires a Conformational Switch in the Pγ C-Terminus. Two sites of an 87-residue rod Pγ subunit, the central polycationic domain (Pγ-24−45), and the C-terminal tail (roughly Pγ-73−87) have been implicated in the binding of Pγ to rod PDEαβ (*6*−*8*, *15*). The C-terminus of Pγ represents a key inhibitory domain (*3*, *4*). To remove this catalytic block and activate PDE, transducin must displace the Pγ C-terminus from the catalytic cavity. The activation of PDE by transducin most likely involves a conformational change in the Pγ C-terminus. A Pγ displacement through simple dissociation from PDEs and

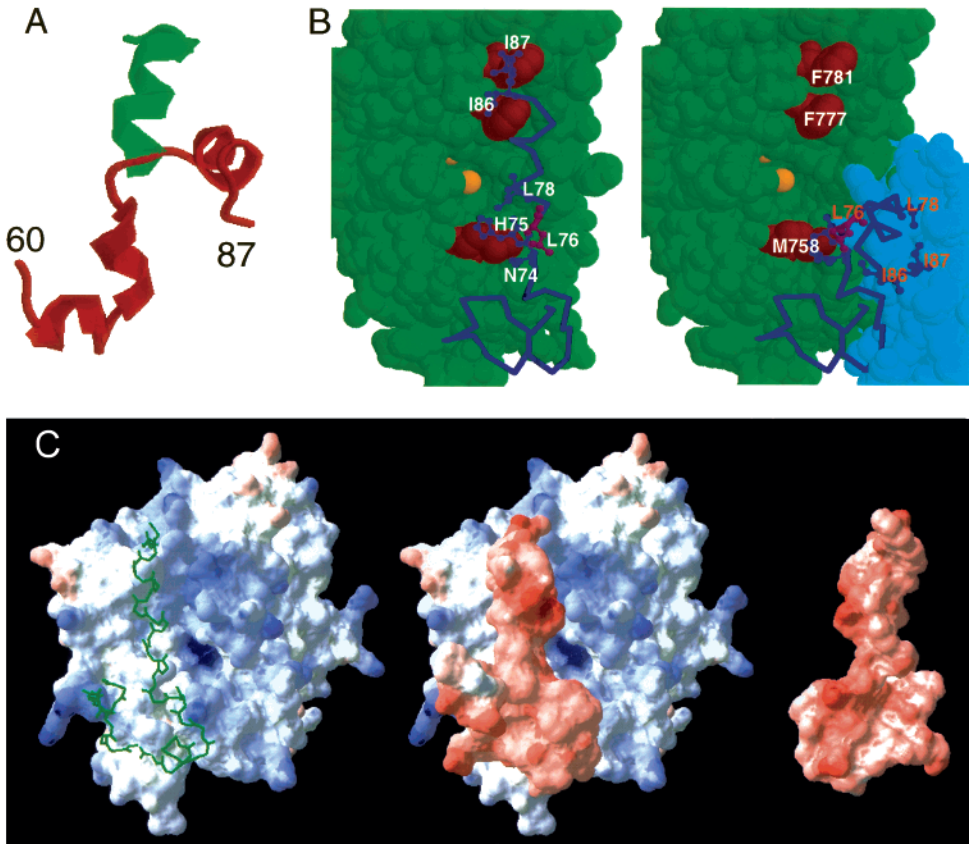

FIGURE 4: Conformational switch in the Pγ C-terminus. (A) Molecular modeling (*33*) shows that Pγ-60−87 undergoes a significant conformational change from the Gtα-bound structure (red) (*5*) upon the extension of helix α3 from residues Pγ-78−83 to Pγ-75−83 (green). (B) At the left is a model of the PDE6α' catalytic domain (a space-filling representation, green) (*5*) with manually docked Pγ-50−87 (a backbone representation, blue) generated using Swiss-PdbViewer (version 3.7b2) (*33*), and the image was obtained using RasMol (version 2.6). The structure of Pγ-50−87 was derived from the crystal structure (*5*) by extending helix α3 to PγHis^{75} and by allowing varying φ and ψ angles for PγGly^{85} and torsion angles of the side chains of Asn^{74}, His^{75}, Ile^{86}, and Ile^{87}. The Pγ C-terminus binding residues (Met^{758}, Phe^{777}, and Phe^{781}) are shown in red. The metal ions (Zn^{2+} and Mg^{2+}) are shown in yellow. The PDE6α' contact residues of Pγ [Asn^{74}, His^{75}, Leu^{78}, Ile^{86}, and Ile^{87} (blue)] and the Gtα contact residue [Leu^{76} (magenta)] are shown in "ball-and-stick" representation. At the right is a model of the transducin-activated PDE6α' complex. The structures of Pγ-50−87 (blue) and Gtα (cyan) are from the structure of the Gtα·Pγ·RGS9 complex (*5*). (C) The molecular surface of the PDE6α'−Pγ-50−87 complex color-coded by electrostatic potential [$-10k_BT$ (red) and $10k_BT$ (blue)] was generated using Swiss-PdbViewer (version 3.7b2) (*33*). At the left is PDE6α', with a view of the active site. Pγ-50−87 is shown in backbone representation. At the center is the PDE6α'−Pγ-50−87 complex. At the right is Pγ-50−87 translated horizontally and rotated 180° about the vertical axis.

subsequent binding to Gtα does not account for the fast activation kinetics (*1*). In the presence of ROS membranes using physiologically relevant protein concentrations, transducin-activated PDE has been shown to be a membrane-bound complex with Gtα (*25*−*27*). Although a direct interaction of activated Gtα with PDE catalytic subunits is likely (*25*, *28*), the complex is held together primarily by Pγ. The polycationic region of Pγ was shown to interact with Gtα (*6*, *7*, *29*) and therefore could serve as a tether. A simultaneous binding of Pγ-24−45 to the PDE catalytic subunit and Gtα in the activated complex would imply that Pγ-24−45 might not undergo a substantial rearrangement upon PDE activation. The structure of the Pγ C-terminal region bound to Gtα has been recently elucidated (*5*). Therefore, the structure of Pγ in complex with PDE6 catalytic subunits holds a key to understanding an activational switch of the effector enzyme.

A Modeling of PDE6−*Pγ Contacts Suggests an α-Helical Conformation of the PDE6-Bound Pγ C-Terminus. Implications for the Gtα-Induced Conformational Switch.* To understand the structure of the Pγ C-terminus in holoPDE, we mapped the point-to-point interactions between Pγ and PDE6α'. This information could be applied to a model of the PDEα' catalytic domain (*11*) to provide distances and constraints for a model of the Pγ C-terminus. The model of the PDEα' catalytic domain was generated previously on the basis of the crystal structure of the PDE4 catalytic domain, which is the first and currently the only available structure of any PDE. The modeled sequence, PDE6α'-518−809, is 57% homologous to the corresponding PDE4 sequence. Therefore, the PDE6α' modeling is appropriate. Recently, a mutational analysis of the Pγ binding site in a chimeric PDE5−PDE6α' enzyme revealed three Pγ contact residues on cone PDE6α': Met^{758}, Phe^{777}, and Phe^{781} (*11*, *12*). The analysis also indicated that Ile^{86} and Ile^{87} of Pγ interact with Phe^{777} and Phe^{781} of PDE6α' (*12*). Furthermore, we suggested that residues adjacent to the PγIle^{86}/Ile^{87} sequence stretch over the catalytic cavity until Pγ reaches the opposite side and contacts PDE6α'Met^{758} (*12*). This study indicates that PγAsn^{74} and/or -His^{75} are probable contact residues of Met^{758}. In agreement with the proposed conformational change, the Gtα-bound structure of the Pγ C-terminus does not allow a fit between Pγ and PDE6α' that would match the contact residues. From a model of the PDE6α' catalytic domain, the distance between Phe^{777} and Met^{758} is ~14 Å. The simplest conformation of the Pγ C-terminus that provides a good

match for the Pγ contact residues is a regular right-handed α-helix. In fact, an α-helix is a preferred conformation for Pγ-75−83 based on the predicted secondary structure (*30*). In the Gtα−Pγ-46−87 complex, PγAsn[74] and -His[75] are situated in the loop between two small α-helices, α2 (Pγ-69−73) and α3 (Pγ-78−83), that run in almost perpendicular planes (*5*). The twist in the polypeptide chain is stabilized by Gtα, which draws contacts with PγLeu[76], -Leu[78], -Leu[81], and -Ile[87]. We hypothesize that in the absence of the Gtα contacts, Pγ-75−83 assumes an α-helical conformation. A molecular model of the Pγ C-terminus suggests that a simple extension of helix α3 to His[75] would eliminate the turn between α2 and α3, and straighten the C-terminus (Figure 4A). This rearrangement would place the Asn[74]/His[75] and Ile[86]/Ile[87] residues in a favorabe position for the interaction with PDE6α′ residues Met[758] and Phe[777]/Phe[781], respectively. Furthermore, the interaction with PDE6α′ is likely to induce and/or stabilize the α-helical conformation of Pγ-75−83. Quite possibly, helices α2 and α3 of Pγ may form a continuous α-helix (Pγ-69−83).

A model of Pγ-50−87 docked to PDE6α′ in a conformation derived from the crystal structure by an extension of helix α3 to residues Pγ-75−83 is shown in Figure 4B. This model requires a certain degree of flexibility for the Ile[86]/Ile[87] residues to enable their interaction with the Phe[777]/Phe[781] residues. The inhibitory defects of the G85A mutant confirm that the rotational freedom provided by Gly[85] to Ile[86]/Ile[87] is important for the inhibition of PDE6 by Pγ. Our Ala-scanning analysis also identified PγLeu[78] as an essential PDE6α′ contact residue. In the model, the side chain of Leu[78] faces the catalytic cavity, and is close to several potential contact residues within the catalytic perimeter. As for Ile[87], Leu[78] participates in the interactions with both PDE and Gtα, further bolstering the mechanism of effector activation through sequestration of the critical Pγ inhibitory residues. Modest reductions in the Pγ affinity for PDE6α′ were observed with the E77A and E80A substitutions. These effects might reflect a contribution of the electrostatic interactions to the Pγ C-terminus−PDE6 binding. The surface surrounding the catalytic pocket is largely neutral to positively charged, whereas the electrostatic potential of the Pγ C-terminus is negative (Figure 4C). Although the model in Figure 4B is in accord with our analysis, it remains speculative as other conformations of the Pγ C-terminus may satisfy the parameters of its binding to PDE6α′ obtained in this study.

How does Gtα induce a switch of the Pγ C-terminus from a proposed "more α-helical" conformation to the bent conformation seen in the Gtα-bound structure? The analysis of transducin activation of reconstituted PDEs containing the C-terminal Pγ mutants with substituted Gtα contact residues provides some interesting clues to the mechanism. The I87A mutation did not cause any significant impairment of Gtα activation. The replacement of the Gtα contact residue in this mutant was probably compensated by a parallel decrease in the affinity of Pγ for the PDE catalytic subunits. Moderate defects in transducin activation resulting from the substitutions of Phe[73], Leu[78], and Leu[81] are consistent with a loss of Gtα contacts. The most severe impairment of the ability of Gtα to activate PDE was observed in the enzyme reconstituted with PγL76A. In the model, the side chain of PγLeu[76] points away from the catalytic pocket and is readily accessible to Gtα (Figure 4B). Leu[76] is also a weak link in the α-helical structure as, together with adjacent residues, it has a relatively low reliability index for an α-helix as a predicted secondary structure (*30*). In addition to PγLeu[76], previous studies (*31*, *32*) and the crystal structure (*5*) implicate PγTrp[70] as a critical residue for the effector activation by transducin. On the basis of the severity of the L76A activation defect, we speculate that GTP-bound Gtα first interacts with Leu[76] and the more N-terminal residues of Pγ, particularly Trp[70]. The interaction with Trp[70] serves to anchor Gtα to the Pγ C-terminus, whereas the interaction with Leu[76] introduces a bend in its α-helical structure. Gtα is then able to engage C-terminal residues Leu[78], Leu[81], and Ile[87] to complete the PDE activation switch of Pγ (Figure 4B).

REFERENCES

1. Chabre, M., and Deterre, P. (1989) *Eur. J. Biochem. 179*, 255−266.
2. Yarfitz, S., and Hurley, J. B. (1994) *J. Biol. Chem. 269*, 14329−14332.
3. Artemyev, N. O., Natochin, M., Busman, M., Schey, K. L., and Hamm, H. E. (1996) *Proc. Natl. Acad. Sci. U.S.A. 93*, 5407−5412.
4. Granovsky, A. E., Natochin, M., and Artemyev, N. O. (1997) *J. Biol. Chem. 272*, 11686−11689.
5. Slep, K. C., Kercher, M. A., He, W., Cowan, C. W., Wensel, T. G., and Sigler, P. B. (2001) *Nature 409*, 1071−1077.
6. Lipkin, B. M., Dumler, I. L., Muradov, K. G., Artemyev, N. O., and Etingof, R. N. (1988) *FEBS Lett. 234*, 287−290.
7. Brown, R. L. (1992) *Biochemistry 31*, 5918−5925.
8. Skiba, N. P., Artemyev, N. O., and Hamm, H. E. (1995) *J. Biol. Chem. 270*, 13210−13215.
9. McAllister-Lucas, L. M., Sonnenburg, W. K., Kadlecek, A., Seger, D., Trong, H. L., Colbran, J. L., Thomas, M. K., Walsh, K. A., Francis, S. H., Corbin, J. D., and Beavo, J. A. (1993) *J. Biol. Chem. 268*, 22863−22873.
10. Granovsky, A. E., Natochin, M., McEntaffer, R. L., Haik, T. L., Francis, S. H., Corbin, J. D., and Artemyev, N. O. (1998) *J. Biol. Chem. 273*, 24485−24490.
11. Granovsky, A. E., and Artemyev, N. O. (2000) *J. Biol. Chem. 275*, 41258−41262.
12. Granovsky, A. E., and Artemyev, N. O. (2001) *J. Biol. Chem. 276*, 21698−21703.
13. Papermaster, D. S., and Dreyer, W. J. (1974) *Biochemistry 13*, 2438−2444.
14. Yamanaka, G., Eckstein, F., and Stryer, L. (1985) *Biochemistry 24*, 8094−8101.
15. Artemyev, N. O., and Hamm, H. E. (1992) *Biochem. J. 283*, 273−279.
16. Gillespie, P. G., and Beavo, J. A. (1988) *J. Biol. Chem. 263*, 8133−8141.
17. Hurley, J. B., and Stryer, L. (1982) *J. Biol. Chem. 257*, 11094−11099.
18. Kleuss, C., Pallast, M., Brendel, S., Rosenthal, W., and Schultz, G. (1987) *J. Chromatogr. 407*, 281−289.
19. Artemyev, N. O., Arshavsky, V. Y., and Cote, R. H. (1998) *Methods 14*, 93−104.
20. Thompson, W. J., and Appleman, M. M. (1971) *Biochemistry 10*, 311−316.
21. Natochin, M., and Artemyev, N. O. (2000) *Methods Enzymol. 315*, 539−554.
22. Bradford, M. M. (1976) *Anal. Biochem. 72*, 248−254.
23. Laemmli, U. K. (1970) *Nature 227*, 680−685.
24. Towbin, H., Staehelin, T., and Gordon, J. (1979) *Proc. Natl. Acad. Sci. U.S.A. 76*, 4350−4354.
25. Catty, P., Pfister, C., Bruckert, F., and Deterre, P. (1992) *J. Biol. Chem. 267*, 19489−19493.
26. Clerc, A., and Bennett, N. (1992) *J. Biol. Chem. 267*, 6620−6627.
27. Malinski, J. A., and Wensel, T. G. (1992) *Biochemistry 31*, 9502−9512.

28. Clerc, A., Catty, P., and Bennett, N. (1992) *J. Biol. Chem. 267*, 19948−19953.
29. Artemyev, N. O., Rarick, H. M., Mills, J. S., Skiba, N. P., and Hamm, H. E. (1992) *J. Biol. Chem. 267*, 25067−25072.
30. Rost, B. (1996) *Methods Enzymol. 266*, 525−539.
31. Otto-Bruc, A., Antonny, B., Vuong, T. M., Chardin, P., and Chabre, M. (1993) *Biochemistry 32*, 8636−8645.
32. Tsang, S. H., Bums, M. E., Calvert, P. D., Gouras, P., Baylor, D. A., Goff, S. P., and Arshavsky, V. Y. (1998) *Science 282*, 117−121.
33. Guex, N., and Peitsch, M. C. (1997) *Electrophoresis 18*, 2714−2723.

BI011127J